Interacting Supernovae: Spectra and Light Curves

33

Sergei Blinnikov

Abstract

The ejecta of a supernova explosion expand with a very high velocity and they immediately impact the circumstellar material. The manifestation of this impact depends mainly on the density of the circumstellar material and on the velocity contrast between the ejecta and that material. We describe the effects of the interaction of supernova ejecta with circumstellar material on the observed spectral features and light curves of supernovae. The most interesting effect of the interaction is the powerful production of light by radiating shock waves. Many superluminous supernovae may be explained by this mechanism. We describe the relevant physical picture for the efficient production of light in those objects, which is most effective when the mass of circumstellar material is large and slowly moving.

Contents

S. Blinnikov (✉)
Institute for Theoretical and Experimental Physics (ITEP), Moscow, Russia

Kavli Institute for the Physics and Mathematics of the Universe (Kavli IPMU), Kashiwa, Chiba, Japan
e-mail: Sergei.Blinnikov@itep.ru

A.W. Alsabti, P. Murdin (eds.), *Handbook of Supernovae*,
https://doi.org/10.1007/978-3-319-21846-5_31

1 Introduction

All supernovae (SN) interact with interstellar matter at some stage. If the density of the nearby matter is not high then this interaction becomes observable only some decades after the explosion as X-rays from a young supernova remnant. In this chapter we concentrate on cases when the density in the vicinity of the exploding star is much higher than average in the interstellar medium.

The interaction of supernova ejecta with circumstellar material (CSM), such as a strong pre-supernova wind or the debris of previous episodes of mass ejection, may lead to periods of enhanced radiation power lasting from hours to months in visible light, the ultraviolet or the infrared, and/or in radio and X-rays, and to peculiarities in the Supernova (SN) spectra (such as narrow lines). This case is called an interacting supernova. In this chapter, we concentrate on the theory of such supernovae. We describe the effects of the interaction of SN ejecta with circumstellar material on spectral features of observed supernovae in Sect. 2. The most interesting effect of ejecta-CSM interaction is the powerful production of light by radiating shock waves, which we discuss in Sect. 3.

2 Interaction Regimes and Spectral Signatures

Historically, the first identification of a supernova-CSM interaction was the discovery of strong radio emission from SN 1979C, which followed an ejecta-wind interaction model (Chevalier 1982b). Here, we concentrate on the manifestations of ejecta-wind interaction in visible light, which are of crucial importance for understanding this phenomenon.

Specific features in the spectra of supernovae may provide earlier evidence of an interaction with a dense circumstellar wind long before the radio emission (if any) becomes detectable; furthermore, spectral line profiles can provide information about the wind morphology (some information may also be extracted also from light curves).

All stars lose mass in the form of stellar winds. If the mass loss is weak, $\dot{M} \sim 10^{-14}\, M_\odot/\mathrm{yr}$ (this value is typical for our Sun), its influence on the supernova outburst can be neglected. For many types of pre-supernova stars the winds may be much more powerful. In addition to quasi-steady winds, other hydrodynamic events such as pulsations, eruptions, and violent mass transfer in a binary star, occurring prior to a SN explosion (Smith 2014), may strongly enhance the density of the circumstellar matter. This may lead to many interesting peculiarities in the observations.

The evaluation of the mass-loss rate, $\dot{M}$, for a pre-supernova star is based on the idealisation of a spherically symmetric wind with velocity u through a sphere of an arbitrary radius r :

$$\dot{M} \equiv \text{Area} \times \text{mass flux density} = 4\pi r^2 \rho(r) u(r). \tag{1}$$

In reality the density and velocity fluctuate at any given r, sometimes greatly, and the measurement of $\dot{M}$ is not an easy task.

The structure of the CSM formed by violent mass ejections before the supernova explosion may be quite complicated. Yet very often it is described in terms of an ideal "wind". A standard idealisation of the steady wind flow for r much larger than the radius R of the star is the assumption that the velocity is constant in space and time. For $u = \text{const}(r)$ and constant $\dot{M}$ we should have from the definition (1):

$$\rho(r) = \frac{\dot{M}}{4\pi r^2 u} \propto r^{-2}. \tag{2}$$

One should remember that the simple law (2) for the flow has a very limited applicability. We can speak safely of a "wind" when the mass-loss rate $\dot{M}$ is weak, like the wind of solar-type stars, $\dot{M} \sim 10^{-14}\, M_\odot$/yr, but those weak winds do not produce observable features in supernova fluxes and spectra. Interesting events occur when the mass-loss rate is much larger: $\dot{M} \gtrsim 10^{-4}\, M_\odot$/yr. For some interacting supernovae, the "wind" interpretation suggests $\dot{M} \sim 1\, M_\odot$/yr. This enormous mass-loss rate cannot be sustained by a pre-supernova star for many years, and the CSM that it generates must terminate near the star. This implies automatically that the "wind" picture is self-contradictory, because it assumes a steady outflow with velocity independent of the distance from the star. In reality, a wind flow with velocity constant in space is impossible if the mass-loss rate is so monstrous.

The wind density parameter

$$w \equiv \frac{\dot{M}}{u} \tag{3}$$

is very useful for direct estimates of density

$$\rho(r) = \frac{w}{4\pi r^2}. \tag{4}$$

The value of w is less than 10^{14} g cm^{-1} for red supergiants. This is more than two orders of magnitude below typical estimates of $w \sim 10^{16}$ g cm^{-1} for SNe IIn and four orders of magnitude below superluminous SNe IIn having $w \sim 10^{18}$ g cm^{-1} (Smith et al. 2009).

Interacting Type II supernovae (SN Type II) show a wide range of properties. The density and temporal characteristics of the CSM for different types of interacting SN Type II have previously been summarised by Chugai (1997b) and Benetti (2000).

In terms of the "wind," the two main parameters that define the characteristics of those events are the mass-loss rate $\dot{M}$ and the type of the wind (uniform or clumpy).

Interacting supernovae have been classified by Turatto (2003). The taxonomy for SN Type II is based on the strength of the CSM-ejecta interaction signatures. Classical SN Type II are the most frequent. Here the emission is determined by the thermal bath in the ejecta whose entropy was raised by the shock wave from the SN explosion. The entropy, and hence light production, may also be raised by a radioactive material, such as ^{56}Ni or ^{56}Co. For these events CSM-ejecta interaction is negligible (at least in the early phases). Very often they are divided into plateau (II-P) and linear (II-L) subtypes depending on the shape of the light curve in the V band. (One should remember that a "linear" light curve is one with a straight line fit for the dependence of magnitude on time, whereas for the flux or luminosity the same physical emission law is the exponential function of time.) The division between II-P and II-L is not sharp and the boundary between II-P and II-L is not clearly defined. It may correspond to a range in the hydrogen envelope masses from $\sim$10 $M_\odot$ in SN Type II-P to $\sim$ 1 $M_\odot$ in II-L. The difference in hydrogen mass could be due to different mass-loss histories and progenitor masses.

Moreover, some supernovae with hydrogen-free spectra, which may be classified like Type I near the maximum light, behave as like Type II on later epochs, when hydrogen is clearly visible, such as SN 2014C (Margutti et al. 2017). See also Nomoto et al. (2005) on SN 2002ic, which was discovered as Type Ia, but showed hydrogen lines later. Similar behaviour has also been seen also for some superluminous supernovae (SLSN) discovered as Type I which may show hydrogen lines a month or so after peak luminosity (Benetti et al. 2014). This demonstrates that the hydrogen envelope can be lost not long before the SN explosion and excited by the shock a bit later.

Along the sequence of interacting SNe discussed in Chugai (1997b), Benetti (2000) and Turatto (2003) in different notations the explosions take place in a progressively more dense CSM, which in turn provides evidence of progressively more intense mass loss by the progenitor stars or other violent events in pre-supernovae. The Type IIn ("n" here denotes narrow emission lines in their spectra) is the most interesting for the theory of interacting supernovae. Type IIn supernovae are thought to happen inside a dense wind $\dot{M} > 10^{-4} u_{10}\, M_\odot$/yr (where u_{10} is the wind velocity in units of 10 km/s), which can be either clumpy or uniform, and what we see is not the explosion itself, but the product of the interaction.

Let us consider the observable signatures of interaction of supernova ejecta with CSM as a function of increasing density of the CSM.

2.1 Rarefied CSM: Absorption Signatures

Ejecta of a supernova explosion expand with a very high velocity. The ejecta immediately impact the circumstellar material. The manifestation of this impact depends mainly on the density of the CSM and on the velocity difference between

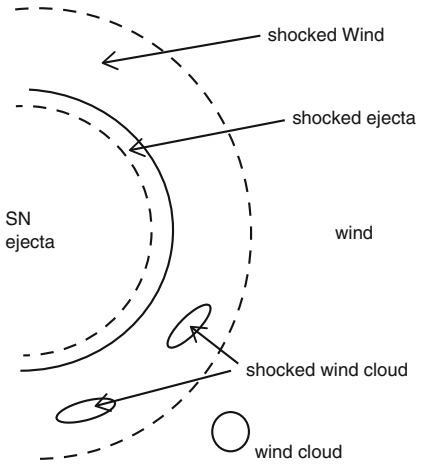

Fig. 1 Schematic view of the interaction of a supernova with the pre-supernova wind. The outer and inner shock waves (*dashed lines*) produce a double-shock structure, with a contact discontinuity (*solid line*) between. Wind clouds (bottom part of the sketch) are crushed by slow shocks driven by the shocked intercloud wind or ejecta (From Chugai 1997a)

the ejecta and the CSM. If the density of the CSM is relatively small, the emission from the CSM-ejecta interaction becomes visible only after the SN has become faint, sometimes several years after the explosion. Many of those events are SNe II-L. This is consistent with the assumption that SNe II-L experience stronger mass loss during their evolution in their pre-supernova lives.

An ejecta-wind interaction is shown schematically in Fig. 1. It shows the major structures both for a spherically-symmetric smooth wind (top quadrant) and a clumpy wind (lower quadrant). The ejecta of a supernova may be thought of as a freely-expanding ($u = r/t$), roughly homogeneous spherical ball with a density cut-off at its outer edge. A supernova in a spherically-symmetric, smooth circumstellar wind creates a standard double-shock wave structure, with a contact discontinuity between (Chevalier 1982b). If the density in the wind is not high, then the forward shock propagating in the wind is fast, hot (T up to $\sim 10^9$ K),and adiabatic. The reverse shock propagating into the supernova envelope is slow and radiative: it creates a thin, cool, dense shell at the contact discontinuity.

Numerous hydrodynamic models for the shock breakout phase predict the formation of a thin dense shell at the outer boundary of the SN ejecta. This is explained by the transition from the adiabatic to the radiative regime of shock wave propagation in the outermost layers of the exploding star. Simple considerations of radiative diffusion (Chevalier 1981) give an estimate for the shell mass:

$$M_s \approx 2 \times 10^{-4} \left(\frac{R}{500\ R_\odot} \right)^2 \left(\frac{u_b}{10^4\ \mathrm{km\ s^{-1}}} \right)^{-1} \left(\frac{\kappa}{0.4\ \mathrm{cm^2\ g^{-1}}} \right)^{-1} M_\odot, \qquad (5)$$

where R is the radius of either the progenitor star or of the dense CSM envelope which may surround the supernova, u_b is the velocity at shock breakout, before free expansion has been established, and κ is opacity of the matter in the shell formation

layers. We see that the shell mass may grow from a tiny fraction of the star mass for ordinary supernovae to several $M_\odot$ in strongly-CSM-interacting SNe embedded into huge massive clouds.

The interaction with a clumpy wind differs from the case of smooth, spherically-symmetric wind in at least one important respect: apart from the main shock wave in the intercloud wind, we also have slow shocks propagating in dense clouds. Shocked clouds may be responsible for the bulk of X-ray and optical emission in some SNe of Type II.

For a very dense "wind" typical for SLSN the picture is different from that presented in Fig. 1. In particular, the forward shock may be radiative as well, and high T is never reached; see Sect. 2.3.

Chugai et al. (2007) proposed diagnostics for circumstellar interaction in Type II-P supernovae by the detection of high-velocity absorption features in Hα and He I 10830 Å lines during the photospheric stage; see Fig. 2.

To demonstrate the method, they computed the ionisation and excitation of H and He in supernova ejecta taking into account time-dependent effects and X-ray irradiation. They found that the interaction with a typical red supergiant wind should result in enhanced excitation of the outer layers of unshocked ejecta and the emergence of corresponding high-velocity absorption, that is, a depression in the blue absorption wing of Hα and a pronounced absorption of He I 10830 Å at a radial velocity of about -10^4 km s^{-1}. They identified a high-velocity absorption

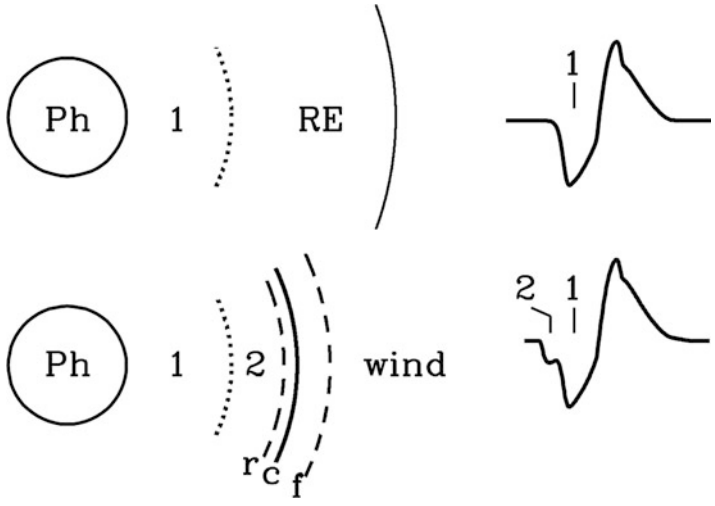

Fig. 2 Schematic picture of the formation of Hα without and with CS interaction. In the absence of CS interaction (*upper diagram*), the absorption component forms in the inner layers of ejecta (1) against the photosphere (Ph); the outer recombined ejecta (RE) do not contribute to the absorption line profile (*upper right*). With CS interaction (*lower diagram*), the double-shocked structure arises at the SN/wind interface with the forward shock (f), reverse shock (r), and contact surface where the cool dense shell occurs (c). The X-rays, primarily from the reverse shock, ionize and excite the layers (2) which produce a depression in the blue wing of the undisturbed absorption (*bottom right*). (From Chugai et al. 2007)

in Hα and He I 10830 Å lines of SN 1999em and in Hα of SN 2004dj as being due to that effect. The derived mass-loss rate was close to $10^{-6}\,M_{\odot}\,\mathrm{yr}^{-1}$ for both supernovae, assuming a wind velocity 10 km s^{-1}.

The evolution of the high-velocity absorption for the classical Type II SN 1999em showed that there is an optimal phase at about the middle of the plateau ($\sim$50 d) when the CS interaction effect is most pronounced. At an early stage (e.g., on day 20) the CS interaction effect was not clearly seen because of the merging of high velocity absorption with the strong undisturbed absorption, whereas at a later stage (e.g., 80 d) high-velocity absorption became very faint.

Some weakly interacting supernovae may have a narrow optical maximum and low luminosity at the stage when the light curve is powered by radioactive decay. The case of a moderate-density wind may correspond to SN 1987B-type supernovae, which show signatures of interaction with a wind and have relatively low luminosity (Schlegel et al. 1996).

The theory developed in Chugai et al. (2007) has been supported by observations of a number of SNe II.

The bright Type II-P SN 2009bw had spectra revealing high-velocity lines of Hα and Hβ until about 3 months after the shock breakout. This suggests a possible early interaction between the SN ejecta and pre-existing circumstellar material (Inserra et al. 2012). Close inspection of the spectra of the Type II-L supernova SN 2013by indicated asymmetric line profiles and signatures of high-velocity hydrogen (Valenti et al. 2015). A very similar Type II-L, SN 2013ej, had weak signs of interaction (Bose et al. 2015). All three objects showed a very fast transition to the tail (nebular) phase and a rather low mass of radioactive ^{56}Ni. The presence of high-velocity features in those Type II SNe can indeed be interpreted as interaction between rapidly expanding SN ejecta and CSM.

For hydrogen-free, weakly interacting supernovae, other predictions for spectral features have been made. Raskin and Kasen (2013) discuss those predictions for SN Type Ia.

SN Type Ia supernovae may be caused by the merger of two white dwarfs. The merger may be preceded by the ejection of some mass from the two stars in "tidal tails," creating a circumstellar medium around the system. The observational signatures from this material depend on the lag time between the start of the merger and the ultimate explosion. If the time lag is fairly short, then the interaction of the supernova ejecta with the tails could lead to detectable shock emission at radio, optical, and/or X-ray wavelengths.

At somewhat later times, the tails produce relatively broad NaID absorption lines with velocity widths of the order of the white dwarf escape speed ($\sim$1000 km s^{-1}). That none of these signatures have been detected in normal SNe Ia constrains the lag time to be either very short ($\lesssim$100 s) or fairly long ($\gtrsim$100 yr). If the tails have expanded and cooled over timescales $\sim 10^4$ yr, then they could be observable through narrow NaID and Ca II H&K absorption lines in the spectra, which are seen in some fraction of SNe Ia. Synthesised NaID line profiles show that, in some circumstances, tidal tails could be responsible for narrow absorptions similar to those observed.

The alternative scenario for SN Type Ia is the explosion of one white dwarf pushed over the Chandrasekhar mass by accretion, the single degenerate scenario. In this case, one may expect a nonnegligible amount of hydrogen to remain unaccreted in the CSM. This question was addressed in a paper (Nomoto et al. 2005) devoted to SN Type Ia showing hydrogen features in their spectra. Among the important issues in identifying the progenitor system of SNe Ia, they focussed mostly on circumstellar interaction in SN 2002ic, and gave a brief discussion on the controversial issues of the effects of rotation in merging double degenerates and steady hydrogen shell burning in accreting white dwarfs.

SN 2002ic was a unique supernova which showed the typical spectral features of SNe Ia near maximum light, but also apparent hydrogen features that have usually been absent in SNe Ia. Based on hydrodynamical models of circumstellar interaction in SN Ia (Nomoto et al. 2005), one may conclude that its circumstellar medium was aspherical (or highly clumpy) and contained $\sim$1.3 $M_{\odot}$.

More intensive stellar winds may blow away not only a hydrogen, but also a helium envelope. As a result, a Type Ibn SN can be produced. Supernovae exploding in a dense CSM are considered in the next section.

2.2 Dense CSM: Emission Lines and Continuum

In addition to some features observed in absorption (see Sect. 2.1) the ejecta-wind interaction gives rise to four major signs (not always observed simultaneously) in the supernova display in visible light (Chugai 1997a):

(i) narrow emission lines from the photoionised undisturbed wind
(ii) broad emission lines from shocked and/or undisturbed photoionised ejecta
(iii) an intermediate emission line component from the shocked wind clouds
(iv) continuum from shocked ejecta or/and wind clumps.

As discussed in Sect. 2.1, if the density of the CSM is relatively small, the emission from CSM-ejecta interaction becomes visible only after the SN has become faint several years after the explosion. At the other extreme, the CSM near the SN may be so dense that the ejecta interact with the wind at early phases and dominate the SN emission. With improved statistics and quality of observations we have now observed counterparts for the different scenarios. Hydrogen-rich supernovae with a strong interaction are called SNe IIn. The ejecta interact with the dense CSM surrounding them soon after the explosion and emission from the SN itself is overwhelmed by the emission arising from the interaction (Grasberg and Nadezhin 1986). Historically, one of the good examples of this class was SN 1988Z. Recently, much more powerful SLSNe have been discovered which are explained by the interaction between the ejecta and a wind.

The most remarkable observational features of Type IIn supernovae known up to now are:

(i) their optical spectrum, dominated by intense emission lines.
(ii) their slow spectral evolution.

(iii) their slow luminosity evolution. sometimes, for several months the flux changes at a rate of only ∼0.004 mag/day (by contrast with classical SNe II-P, U and B fluxes decline as slowly as the V-band).
(iv) Furthermore, some of these supernovae (but not all) are among the most powerful radio supernovae and/or X-ray emitters.
(v) Finally, there are some indications that Type IIn SNe have an IR excess, due to dust formation.

The interaction of the ejecta of a supernova explosion with the dense circumstellar medium plays a significant role in the output energy of these Type IIn supernovae. This interaction produces a radiative shock which becomes more and more important as the density of the CSM increases. For number densities of the order of $\sim 10^7$ cm^{-3}, it is the dominant physical process.

Direct measurements of the CSM in SNe IIn are possible thanks to high-resolution spectra (better than 10 km/s), provided by echelle spectrographs: for example, for early work see Salamanca (2003), and more recently Kankare et al. (2012). Echelle spectra of Type IIn SN show a very narrow P Cygni line atop the broad emission lines H_α and H_β. These narrow P Cygni profiles originate in the dense and slowly expanding ($u \sim 100$ km/s) medium into which the SN shock progresses. This points to a massive and slow wind of the progenitor just before its explosion as a supernova. If such material is created by a wind not long before the explosion, then the mass-loss rate must be of the order of $10^{-2} M_\odot$ yr^{-1} or higher. This value is much larger than the typical mass-loss rate of the winds of OB stars, or indeed yellow and red supergiants.

Leloudas et al. (2015) simulated spectra making the transition from SN Type Ia to SN Type IIn (with growing density of CSM). They constructed spectra of supernovae interacting strongly with a circumstellar medium in a simplified model by adding SN templates, a black-body continuum, and an emission-line spectrum. A more advanced simulation taking account of radiative transfer supports the simple model as a good first-order approximation.

In a Monte Carlo simulation a large number of parameters are varied, such as the SN type, luminosity and phase, the strength of the CSM interaction, the extinction, and the signal-to-noise ratio (S/N) of the observed spectrum.

Leloudas et al. (2015) used Monte Carlo methods to generate more than 800 spectra, and distributed them to 10 different people for classification. They studied how the different simulation parameters affected the appearance of the spectra and therefore their classification. SNe Type IIn showing some structure over the continuum were characterised as "SNe IInS" to allow for a better quantification. It was demonstrated that the flux ratio of the underlying SN to the continuum f_V is the single most important parameter determining whether a spectrum can be classified correctly. Other parameters, such as extinction, S/N, and the width and strength of the emission lines, do not play a significant role.

In the simulation, thermonuclear SNe were progressively classified as Ia-CSM, IInS, and IIn as f_V decreased. The transition between Ia-CSM and IInS occurs at $f_V \sim 0.2$–0.3. It was therefore possible to determine that SNe Ia-CSM are found at the absolute magnitude range $-19.5 > M > -21.6$ (extinction corrected), in very

good agreement with observations, and that the faintest SN IIn that can hide a SN Ia has $M = -20.1$.

"91T-like" superluminous supernovae of Type Ia (named after the bright supernova SN 1991T) show at early times weak silicon and calcium lines, leading to a nearly featureless continuum. The literature sample of SNe Ia-CSM shows an association with 91T-like SNe Ia. Leloudas et al. (2015) studied whether this association could be attributed to a luminosity bias (91T-like being brighter than normal events), but the data suggest the association is real, with underlying physical origins. It is proposed that 91T-like explosions result from single degenerate progenitors that have earlier generated their CSM.

Despite the spectroscopic similarities between SNe Ibc and SNe Ia, the number of misclassifications between these types was very small in the simulation by Leloudas et al. (2015) and mostly when the spectra had low signal-to-noise ratios. Combined with the SN luminosity function needed to reproduce the observed SN Ia-CSM luminosities, it is unlikely that SNe Ibc constitute an important contaminant within this sample. Leloudas et al. (2015) show how Type II spectra transition to IIn and how the Hα profiles vary with f_V. SNe IIn fainter than $M = -17.2$ are unable to mask SNe II-P brighter than $M = -15$. The spectra obtained are in good agreement with real data.

Another way to find the history of mass loss of pre-supernovae is to study the bolometric light curves of the SNe. The shape of light curves must depend on the interaction of ejecta and CSM. Moriya et al. (2014) presented results of a systematic study of the mass-loss properties of Type IIn supernova progenitors over the decades before their explosion. An analytic light-curve model was applied to 11 Type IIn supernova bolometric light curves to derive properties of their circumstellar medium. A detailed comparison between the analytic predictions and detailed numerical radiation hydrodynamic simulations supported the results. The mass-loss histories were reconstructed based on the estimated CSM properties.

The estimated mass-loss rates were mostly higher than $10^{-3}\ M_\odot\ \mathrm{yr}^{-1}$, consistent with those obtained by other methods. The mass-loss rates were often found to be constantly high for decades prior to the explosion. This indicates that there exists some mechanism to sustain the high mass-loss rates of Type IIn supernova progenitors for this time. Thus, the shorter, eruptive mass-loss events observed in some progenitors of Type IIn supernova are not always responsible for creating their dense circumstellar media. In addition, it is found that Type IIn supernova progenitors may tend to increase their mass-loss rates as they approach the time of their explosion.

Massive stars exploding in a He-rich circumstellar medium produce Type Ibn supernovae, that is, hydrogen-free, helium-rich supernovae showing narrow lines. A good example was SN 2014av, the spectra of which were studied by Pastorello et al. (2016). The spectra were initially characterised by a hot continuum. Later on, the temperature declined and a number of lines became prominent mostly in emission. In particular, later spectra were dominated by strong and narrow emission features of HeI typical of Type Ibn SNe, although there was a clear signature

of lines from heavier elements (in particular OI, MgII, and CaII). A forest of relatively narrow FeII lines was also detected showing P-Cygni profiles, with the absorption component blue-shifted by about 1200 km s^{-1}. Another spectral feature often observed in interacting SNe, a strong blue pseudo-continuum, was seen in the latest spectra of SN 2014av.

Another example was the peculiar Type Ib SN 2006jc (Foley et al. 2007; Pastorello et al. 2007), with good optical photometry and spectra. Strong and relatively narrow He I emission lines indicated that the progenitor star exploded inside a dense circumstellar medium (CSM) rich in He. An exceptionally blue apparent continuum persisted from the first spectrum, obtained 15 days after discovery, through to the last spectrum ∼1 month later. One or two of the reddest He I line profiles in the spectra were double-peaked, suggesting that the CSM has an aspherical geometry. The He-rich CSM, aspherical geometry, and line velocities indicate that the progenitor star was an early-type (hot massive) Wolf–Rayet star (W–R star) of spectral class WNE. Two years before the SN, a luminous outburst similar to those seen in luminous blue variables (LBVs) was observed. This event is suspected to have produced the dense CSM. Such an eruption associated with a W–R star had not been seen before, indicating that the progenitor star may have recently transitioned from the LBV phase.

2.3 Cool Dense Shell Fragmentation and CSM Lumpiness

For, a very dense "wind" typical of SLSN, the pattern of the flow is different from that presented in Fig. 1. The velocity profiles show a multireflection structure which forms from the very beginning of the ejecta–wind interaction. The structure evolves very quickly to the standard two-shock (forward and reverse) picture. This does not depend on the initial velocity profile in the envelope. Very crudely the evolution looks like a self-similar behaviour analogous to the Nadyozhin–Chevalier solution (Chevalier 1982a; Nadezhin 1985). However, due to high density, both forward and reverse shocks are radiative and they merge, forming the dense shell; see Fig. 3. The thin dense shell with a very large radius would most probably be unstable and fragment into smaller lumps. This in turn leads to the flow becoming essentially multidimensional.

Theoretical studies of the stability of those cool dense shells (CDS) are still at an early stage of development. Nevertheless, the analysis of observations leads to certain conclusions on CDS fragmentation.

Chugai (2009) has shown that fragmentation of CDS helps to explain peculiar properties of the light curves and continua of enigmatic Type Ibn supernovae, and argued in favour of early strong circumstellar interaction. This interaction explains the high luminosity and short rise time of SN 1999cq, and the cool dense shell formed in shocked ejecta can explain the smooth early continuum of SN 2000er and unusual blue continuum of SN 2006jc (Type Ibn). The dust was shown to condense in the CDS at about day 50. Monte Carlo modelling of the HeI 7065 Å line profile

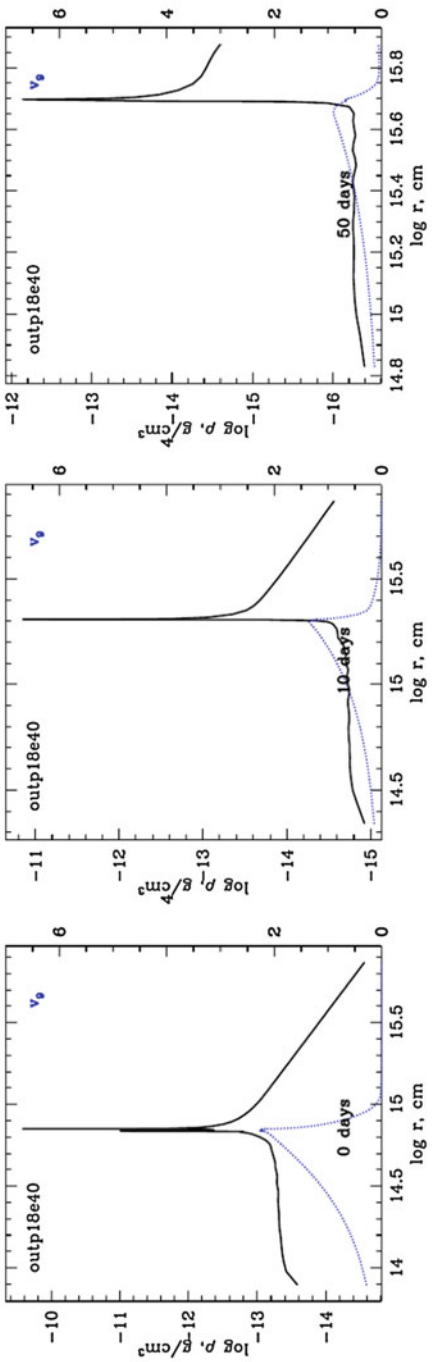

Fig. 3 Long-living dense shells (Sorokina et al. 2016)

affected by the dust occultation supported a picture in which the dust resides in the fragmented CDS, whereas HeI lines originate from circumstellar clouds shocked and fragmented in the forward shock wave; see Fig. 1.

The fragmentation of the CDS formed in SNe II-P (see Eq. (5) for the estimate of the shell mass) may help to understand some properties observed in these classical objects. Utrobin and Chugai (2015) studied the well-observed Type II-P SN 2012A with hydrodynamic modelling. They used the early hydrogen Hα and Hβ lines as clumpiness diagnostics: the presence of clumps explained the ratio of those spectral lines. Hydrodynamic simulations showed that the clumpiness modified the early light curve and increased the maximum velocity of the outer layers.

3 Supernovae Powered by Collision of Massive Shells

There are strong arguments to believe that SN Type IIn are powered by collisions of SN ejecta with massive shells (leftover from previous explosions) surrounding the star.

The idea of producing a large radiative flux during the interaction of the gas ejected in subsequent explosions was suggested by Grasberg and Nadezhin (1986) as an explanation of SNe IIn. A physical mechanism for those multiple explosions (pulsational pair instability) was proposed by Heger and Woosley (2002). Woosley et al. (2007) employed this model to explain the Type II superluminous SN 2006gy as a moderately energetic explosion ($\sim 3 \cdot 10^{51}$ ergs) without any radioactive material.

3.1 Multiple Shell Ejection by Massive Stars

Pulsational pair instability (Heger and Woosley 2002) is a physically justified mechanism for producing multiple ejections of shells in the pre-supernova evolution of massive stars. The main uncertainty in those models is the mass-loss rate, especially at stages close to the final SN explosion. Models explored in Woosley et al. (2007) with initial masses $M < 240\ M_\odot$ retained a sufficient mass of hydrogen to produce SNe IIn.

More massive stars with initial masses of 140, 200, and 250 $M_\odot$ and having a metallicity Z = 0.004 were considered in Yoshida et al. (2016). Those stars lose all their hydrogen and a large fraction of their helium layer. Still they have CO cores of $\sim$40–60 $M_\odot$ and they experience pulsational pair-instability (PPI) after carbon burning. This instability induces strong pulsations of the whole star and a part of the outer envelope is ejected. During the PPI period of $\sim$1–2000 years, they experience several pulsations.

The larger CO-core model has the longer PPI period and ejects the larger amount of mass. In as much as almost all surface He is lost by the pulsations, these stars become Type Ic supernovae when they explode. The interaction between the

circumstellar shell ejected by PPI and the supernova ejecta can be an origin of Type I superluminous supernovae.

The PPI is good mechanism for massive stars but it cannot work for stars with initial mass appreciably less than $\sim 100\, M_\odot$ simply because their evolutionary tracks on the $\rho_c - T_c$ diagram never reach the region of pair-creation. However, there are many examples of interacting supernovae which had progenitors of modest masses. That is why one should look for other paths for massive shell ejections. Because many stars are members of binary systems, the effects of binary evolution may play an important role in forming dense CMS in pre-supernovae.

Interacting supernovae, including SNe IIn and SLSNe, appear to have lost perhaps several solar masses of their envelopes in tens to hundreds of years before the explosion. In order to explain the close timing of the mass-loss and supernova events, Chevalier (2012) explores the possibility that the mass loss is driven by common envelope evolution of a compact object (neutron star or black hole) in the envelope of a massive star. The supernova is then triggered by the inspiral of the compact object into the central core of the companion star. The expected rate of such events is smaller than the observed rate of Type IIn supernovae, but the rates are uncertain and might be reconciled.

The velocity of mass loss is related to the escape velocity from the common envelope system and is comparable to the observed velocity of hundreds of kilometres per second in Type IIn events. Some supernovae of this type show evidence of energies in excess of the canonical 10^{51} erg, which might be the result of explosions from rapid accretion onto a compact object through a disk.

A somewhat similar scenario of a neutron star merging with a red supergiant is put forward by Barkov (2012). One of the ensuing SN explosions may be of the interacting type. A magnetar with a millisecond period may also be formed and produce a superluminous event of another type.

Justham et al. (2014) found paths to relate luminous blue variables and Superluminous Supernovae (SLSNe) with binary mergers. Observational evidence suggests that the progenitor stars of some core-collapse supernovae (CCSNe) are luminous blue variables (LBVs), perhaps including some Type II SLSNe. They examined models in which massive stars gain mass from a companion soon after the end of core hydrogen burning.

The post-accretion stars spend their core helium-burning phase as blue supergiants, and many examples are consistent with being LBVs at the time of core collapse. Other examples are yellow supergiants at explosion. The rate of appropriate binary mergers may match the rate of SNe with immediate LBV progenitors; for moderately optimistic assumptions (Justham et al. 2014) estimate that the progenitor birth rate is ~ 1 % of the CCSN rate.

A strong stellar mass loss during the final years before core collapse may be caused by effects which are as yet unexplored in detail. One proposal (Shiode and Quataert 2014) is that internal gravity waves are excited by core convection, enhance the core fusion power, and transport a super-Eddington energy flux out to the stellar envelope, driving mass loss. Another (Moriya 2014) is that the core mass decreases due to neutrino losses and ensuing mass ejection.

3.2 Interaction with Radiation Trapping Effects

The most important effect in the physics of interacting supernovae is the production of a powerful flux of light from the collision of fast-moving ejecta with the dense CMS.

Let us make an estimate. Using standard notations:

$$L = 4\pi\sigma T_{\rm eff}^4 R_{\rm ph}^2. \tag{6}$$

For a supernova at age $t = 10$ d, with typical velocity at the level of the photosphere $u = 10^9$ cm/s (i.e., 10^4 km/s), we get $R_{\rm ph} = ut \approx 10^{15}$ cm. For a typical $T_{\rm eff} \sim 10^4$ K, then $L \sim 10^{43}$ erg/s. The luminosity L goes down over a timescale of some weeks. Thus, in "standard" SN explosions, ordinary, noninteracting supernovae produce $\sim 10^{49}$ ergs in photons during the first year after the explosion.

An energy of $\sim 10^{51}$ ergs remains as kinetic energy of the ejecta. This energy is radiated by the supernova remnant (mostly as X-rays) much later, during the millennia after the explosion. The energy is produced in the shocks produced by ejecta interacting with the ordinary interstellar medium, which has a number density ~ 1 cm^{-3}. If the density of the CSM is $\sim 10^9$ times higher, then a large fraction of the kinetic energy will be radiated away much faster, on a timescale of a year. We may have the same typical $T_{\rm eff} \sim 10^4$ K, so the photons will be much softer than X-ray, emitted mostly in the visible or ultraviolet range. However, $R_{\rm ph} \sim 10^{16}$ cm is much larger and the luminosity goes up approaching $L \sim 10^{45}$ erg/s for some period of time. Thus a superluminous supernova (SLSN) can be produced with the explosion energy on the standard scale of 1 foe $\sim 10^{51}$ ergs, but a major fraction of this energy is lost during the first year.

Let us give some further simple estimates, instead of writing down full systems of hydrodynamic equations (the reader may find some useful detailed formulas in Sect. 4).

If we have a blob of matter with mass m_1 and momentum $\mathbf{p_1}$ its energy is

$$E_1 = \frac{\mathbf{p_1}^2}{2m_1}. \tag{7}$$

If it is colliding with another blob with mass m_0 and zero momentum we get for the final energy of two merged blobs in a fully inelastic collision

$$E_2 = \frac{\mathbf{p_1}^2}{2(m_1 + m_0)}. \tag{8}$$

The momentum is conserved, but because $E_2 < E_1$, an energy $E_1 - E_2$ is lost and radiated away. If $m_0 \ll m_1$ only a tiny fraction of E_1 is radiated, but if $m_0 \gg m_1$, then $E_2 \ll E_1$ and almost all initial E_1 is radiated away.

This means that collisions of low mass, fast-moving ejecta with heavy (dense), slowly-moving blobs of CSM are efficient in producing many photons. Of course one should remember that the momentum of the two merged blobs may be different

from the initial $\mathbf{p_1}$ if we have a directed flux of newborn photons which carry some net momentum away. There is not much sense in evaluating this effect using the order-of-magnitude estimates because details of the production of photons may be complicated. The degree of "inelasticity" of the collision depends on the pattern of hydrodynamic flow and on the properties of emission/absorption of the plasma, for example, on its composition. However, these details and an accurate account of the conservation of momenta and energy must be covered in full radiation hydrodynamic simulations.

Now let us estimate simply the temperature behind the shock front. The pressure behind the shock front is P_s where we have

$$P_s \sim \rho_0 D^2 = n_0 m_i D^2 \tag{9}$$

if the density upstream of the front is ρ_0, and D is the velocity of the front. The density $\rho = n m_i$ with n the number density and m_i the average mass of the ions. The estimate (9) follows from momentum conservation: the momentum flux is $P + \rho u^2$ for the flow having velocity u. P is negligible ahead of the front where the matter is cold. A more accurate expression for P_s is given in Sect. 4, Eq. (11).

The estimate (9) gives for a nonrelativistic plasma with pressure $P = n k_B T$:

$$k_B T_s \sim m_i D^2 \tag{10}$$

which suggests very high temperatures, in the keV range, and higher for shock velocities larger than a thousand km/s. For exact coefficients see Eq. (13) in Sect. 4.

We do not give numerical estimates for these quantities here because in many cases in supernova envelopes they are misleading. In reality, the plasma in supernova conditions is at least partly relativistic: we have a huge number of photons with $P = aT^4/3$, and so T_s is appreciably lower due to the high heat capacity of photon gas. Equations (17) and (18) in Sect. 4 show that, taking account of radiation and with D of order of a thousand km/s and $\rho \sim 10^{-12}$ g $\cdot$ cm^{-3}, we have $T_s = 4.3 \times 10^4$ K, well below the X-ray range of temperatures, but high enough to support a high L for a long time at large R.

3.3 Hydrodynamical Evolution in Synthetic Models

Now we describe some results of numerical simulations which take into account radiation trapping effects in interacting supernovae. For illustration we use the results from Sorokina et al. (2016).

The simulations use pre-supernovae structures obtained either from evolutionary codes or artificially constructed. In any case, the initial models have a fast moving part which may be called "ejecta." This part has mass $M_{\rm ej}$ and radius $R_{\rm ej}$. $M_{\rm ej}$ can be much less than the total mass of the collapsing core; it is just a convenient form of parametrisation of models.

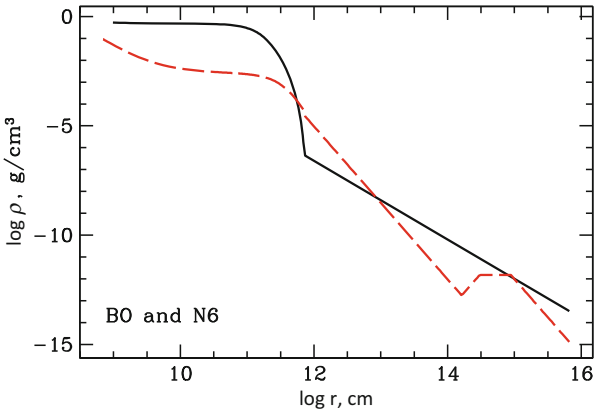

Fig. 4 Two typical examples of the initial density structures for interacting supernovae. The *solid line* shows a windlike model. The *dashed line* shows a model with a detached shell

To make an interacting model the ejecta are surrounded by a rather dense envelope, a "wind," with mass M_w extended to the radius R_w. The outer radius of this envelope must be large $\sim 10^{16}$ cm, or even larger for extreme cases. The envelope may have a power-law density distribution $\rho \propto r^{-p}$, which simulates the wind that surrounds the exploding star.

For a steady wind, $p = 2$. However, in the very last stages of the evolution of a pre-supernova star the wind may not be steady and the parameter p may vary in the range between 1.5 and 3.5. Another kind of envelope, detached from the ejecta by a region of lower density, is also considered. The density distributions for a couple of typical models are shown in Fig. 4.

Light curves are calculated for SNe exploding within these envelopes. A shock wave forms at the border between the ejecta and the envelope. The shock very efficiently converts the energy of the ordered motion of expanding gas to that of the chaotic thermal motion of particles, whose energy can easily be radiated. As a result, one may expect to obtain light curves powerful enough to explain at least a part of superluminous SNe without an assumption of unusually high explosion energy. The detailed computations support those expectations.

For Type IIn SLSNe, hydrogen-rich envelopes are used. For SLSN I, typically carbon-oxygen models with different C to O ratios or helium models are employed. The models may contain some amount of radioactive elements such as ^{56}Ni, but it is not necessary in this class of simulations in as much as the effect of pure ejecta-CSM interaction is sufficient to explain the majority of SLSNe, with zero amount of ^{56}Ni.

The synthetic light curves in Sorokina et al. (2016) are calculated using a multigroup radiation hydrodynamic code STELLA in its standard setup. The code simulates spherically symmetric hydrodynamic flows coupled with multigroup radiative transfer. The opacity routine takes into account electron scattering, free-

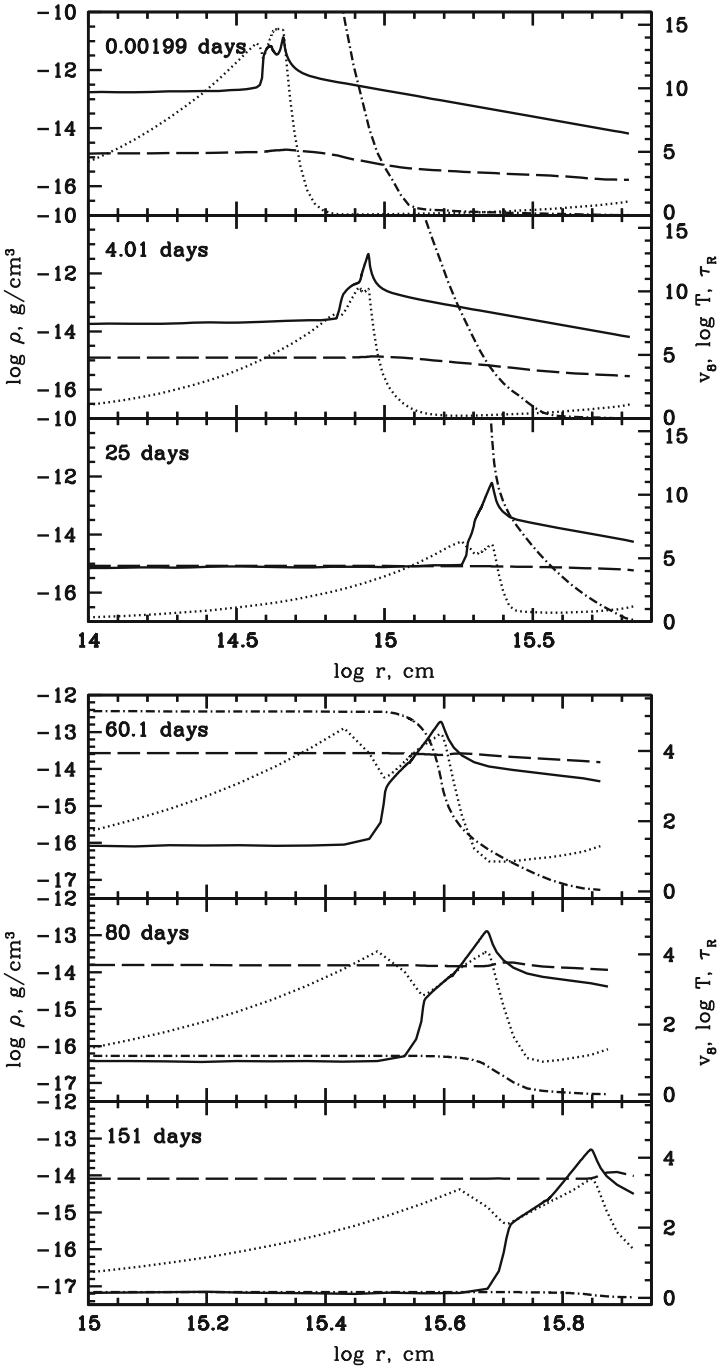

Fig. 5 (Continued)

free and bound-free processes. The contribution of spectral lines (i.e., bound–bound processes) is treated in an approximation of "expansion" opacity.

The explosions have been simulated as a "thermal bomb" with variable energy $E_{\rm expl}$ of the order 2–4 foe, which is a bit larger than in a standard 1 foe supernova, but much lower than invoked in hypernovae or in pair-instability supernovae.

Figure 5 shows how the profiles of density, velocity, temperature, and Rosseland mean optical depth evolve along time for one of the models. The upper panels correspond to the evolution before maximum of the light curve (which happens on day 22 after the explosion for that model). The lower panels show the evolution after maximum.

At the very beginning, the shock wave structure starts to form due to collision between the ejecta and the CSM. Then the emission from the shock front heats the gas in the envelope, thus making it opaque, and the photosphere moves to the outermost layers rather quickly. When the photospheric radius reaches its maximum, one can observe maximal emission from the supernova. The speed of the growth of the photospheric radius depends on the mass of the envelope, because more photons must be emitted from the shock to heat larger mass envelopes.

Another parameter which impacts the initial growth of the photospheric radius is the chemical composition of the envelope. For example, the light curve rises faster for a CO envelope than for a He one, because a lower temperature is needed to reach high opacity in a CO mixture. This light curve behaviour can help set the composition for some observed SLSNe.

The plots on the lower part of Fig. 5 show the stages when the photosphere slowly moves back to the centre, and the envelope and the ejecta finally become fully transparent. At the beginning of this post-maximum stage all gas in the envelope is already heated by the photons which came from the shock region and diffused through the envelope to the outer edge. The whole system (ejecta and envelope) becomes almost isothermal. The shock becomes weaker with time and emits fewer photons which can heat up the envelope, therefore the temperature of the still unshocked envelope falls.

The shocked material is gathered into a thin dense layer (see Fig. 3), which finally contains almost all mass in the system. Formation of this layer leads to numerical difficulties, which significantly limit the timestep of the calculation. Another problem can also take place due to the thin layer formation: a thin dense shell with a very large radius would most probably be unstable and can fragment into smaller lumps. Then the problem would become multidimensional.

Fig. 5 Evolution of radial profiles of the density (*solid lines*), velocity (in 10^8 cm s^{-1}, *dots*), matter temperature (*dashes*), and Rosseland optical depth (*dash-dots*) for one of the models in Sorokina et al. (2016). The scale for the density is on the left y-axis, for other quantities, on the right y-axis. *Upper panels*: evolution of the hydrodynamical structure before maximum; very soon after the explosion and at days 4 and 25. *Lower panels*: the same parameters, but after maximum; at days 60, 80, and 151. Note that different scales for the axes are used on the left and right panels

On the velocity profiles, the multireflection structure forms from the very beginning. It evolves very quickly to the standard two-shock (forward and reverse) picture. This does not depend on the initial velocity profile in the envelope. The interaction of the ejecta with the envelope leads to similar final velocity structures. The behaviour looks self-similar, analogous to the solution found by Nadezhin (1985) and Chevalier (1982a) but with radiation.

3.4 General Properties of the Interacting SLSN Light Curves: From Visible Light to X-Ray

Many properties of SLSN light curves may be explained by a pure effect of interaction with the CSM, without ^{56}Ni or any other additional energy source inside the models. All the emission comes from the transformation of ordered particle motion into a chaotic state when gas passes through a shock wave. When the shock reaches the outer edge of the extended envelope and there is no material in front of the shock any more, then no source of energy remains. The gas loses its thermal energy through radiation and cools down very quickly. This corresponds to a sharp drop in flux in all spectral bands. This drop is a typical feature of the light curves for the interacting models, though it is not always observed because it happens a few months after maximum (if the envelope is extended enough) and the supernova may be unobservable, or another energy source (such as radioactivity) may dominate at this phase.

One clearly needs a very large radius envelope to produce an extremely bright and long-lasting event for a model without a huge explosion energy. One also needs high densities for strong production of light by the shock (see the estimates in Sect. 4). But when the density is too high, the mass of the envelope and the optical depth of the shell become too large. This would make the supernova appear red and would not match with observations of SLSNe-I, which tend to be blue; see, for example, Quimby et al. (2011). Thus an enhanced envelope mass must be accompanied by an enhanced explosion energy which will lead to the formation of stronger and hotter shocks.

Figure 6 demonstrates how the model with hydrodynamic evolution shown in Fig. 5 reproduces multiband observations of the well-studied SLSNe SN 2010gx. The general trend is described very well by the interacting model. One should point out the parallel behaviour of fluxes in different filters for a long time near the maximum light. This is a general property of shocks producing light and their velocity is more or less constant in slowly-varying density.

Analysis of X-ray emission associated with SNe IIn allows us to draw some conclusions on the structure of CSM around those supernovae. In many cases X-rays appear after the flux in visible bands goes down. This is natural, because while the shock is buried within the dense layers its temperature cannot be high (see Eq. 18).

The X-ray emission resulting from the ejecta-CSM interaction depends, among other parameters, on the density of this medium, and therefore the variation in the X-ray luminosity can be used to study the variation in the density structure of the

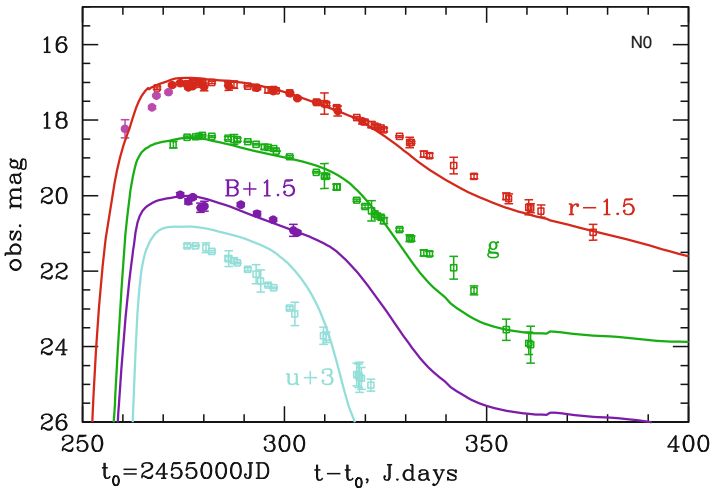

Fig. 6 Synthetic light curves for the model from Fig. 5, one of the best for SN 2010gx, in r, g, B, and u filters compared with Pan-STARRS and PTF observations. Pan-STARRS points are designated with open squares (u, g, and R bands), and PTF points, with *filled circles* (B and r bands). *Four pink points* in the beginning of the r band show PTF observations in the Mould R-band which is similar to the SDSS r band

medium. Dwarkadas (2011) and Dwarkadas and Gruszko (2012) explore the X-ray emission and light curves of all known supernovae, in order to study the nature of the medium into which they are expanding. It was found that in the context of the theoretical arguments that have generally been used in the literature, many young SNe, and especially those of Type IIn SNe, which are the brightest X-ray luminosity class, do not appear to be expanding into steady winds.

Some Type IIn SNe appear to have very steep X-ray luminosity declines, indicating that the density declines much more steeply than r^{-2}. However, other Type IIn SNe show a constant or even increasing X-ray luminosity over periods of months to years. Many other SNe do not appear to have declines consistent with expansion in a steady wind. SNe with lower X-ray luminosities appear to be more consistent with steady wind expansion, although the numbers are not large enough to make firm statistical comments. The numbers do indicate that the expansion and density structure of the circumstellar medium must be investigated before assumptions can be made of steady wind expansion. Unless a steady wind can be shown, mass-loss rates deduced using this assumption may need to be revised.

Many other types of interacting supernovae are X-ray emitters. A classic example is SN 1979C of Type II-L. Immler et al. (2005) presents the long-term X-ray lightcurve, constructed from all the X-ray data available, which reveals that SN 1979C was still radiating at a flux level similar to that detected by *ROSAT* in 1995, showing no sign of a decline in a period of 16–23 years after its outburst. The high inferred X-ray luminosity ($L_{0.3-2} = 8 \times 10^{38}$ ergs s^{-1}) is caused by the interaction of the SN shock with dense circumstellar matter, likely deposited by a

strong stellar wind from the progenitor ($v_w \approx 10$ km s^{-1}) with a high mass-loss rate of $\dot{M} \approx 1.5 \times 10^{-4}\ M_\odot$ yr^{-1}.

The peculiar Type Ib SN 2006jc has been observed with the UV/Optical Telescope (UVOT) and X-Ray Telescope (XRT) on board the Section observatory over a period of 19–183 days after the explosion (Immler et al. 2008). Signatures of interaction of the outgoing SN shock with dense circumstellar material were detected, such as strong X-ray emission ($L_{0.2-10} > 10^{39}$ erg s^{-1}) and the presence of Mg II 2800 Å line emission visible in the UV spectra. In combination with a *Chandra* observation obtained on day 40 after the explosion, the X-ray light curve is constructed, which shows a unique rise of the X-ray emission by a factor of ∼5 over a period of ∼4 months, followed by a rapid decline. They interpret the unique X-ray and UV properties as a result of the SN shock interacting with a shell of material that was deposited by an outburst of the SN progenitor 2 years prior to the explosion.

These results are consistent with the explosion of a Wolf–Rayet star that underwent an episodic mass ejection qualitatively similar to those of luminous blue variable stars prior to its explosion. This led to the formation of a dense ($\sim 10^7$ cm^{-3}) shell at a distance of $\sim 10^{16}$ cm from the site of the explosion, which expands with the WR wind at a velocity of (1300 ± 300) km s^{-1}.

Interacting supernovae which are not very luminous, such as SN 2006jc (Immler et al. 2008) or SN 2009ip, were observed in X-rays near maximum light (Margutti et al. 2014). More luminous ones have been discovered in the X-ray range much later for an obvious reason: they have the high column density needed to produce many visible photons in radiating shocks and the high-density shells would screen X-rays even if they were produced. Another reason for the lack of powerful X-ray emission in SLSNe was already given: it is the low temperature of the shocked matter in radiation-dominated shocks.

An interesting example illustrating this is SN 2010jl. Optical to hard X-ray observations reveal an explosion embedded in a 10 solar mass cocoon (Chandra et al. 2015; Ofek et al. 2014). The growth of X-ray flux began with the decline of the visible flux which should be related with the shock leaving the dense layers of the envelope surrounding the supernova.

4 Strong Shock Waves with Internal Energy (e.g., Ionisation) and Radiation

In this section we derive some of the properties of strong shock waves, pointing out some of the idealisations which are usually made.

We use standard notations for density ρ, velocity u, pressure P, and thermodynamic energy E, and define a vector $\mathbf{U}$ with components:

$$U_1 = \rho,$$

the density of the momentum

$$U_2 = \rho u \equiv j,$$

and the total energy density

$$U_3 = E + \frac{\rho u^2}{2}.$$

We also define a vector $\mathbf{F}$ having as components the flux of mass,

$$F_1 = \rho u,$$

the flux of momentum,

$$F_2 = \rho u^2 + P,$$

and the flux of energy

$$F_3 = (E + \frac{\rho u^2}{2} + P)u,$$

and we have a general law of conservation:

$$\frac{\partial \mathbf{U}}{\partial t} = -\frac{\partial \mathbf{F}}{\partial x}.$$

In a stationary case, that is, $\partial \mathbf{U}/\partial t = 0$, we get $\mathbf{F} = \text{const}$. We have already introduced above a standard notation for the flux of mass, j, and we see now that it is constant in a stationary flow:

$$j \equiv \rho u = \text{const}.$$

It is convenient to use a specific volume (per unit mass):

$$V \equiv \frac{1}{\rho}\ .$$

From $F_2 = \rho u^2 + P = j^2 V + P = \text{const}$ we obtain:

$$j^2 V_0 + P_0 = j^2 V_s + P_s\ ,$$

And this implies:

$$P_s = P_0 + j^2 (V_0 - V_s)\ .$$

The subscript "0" for $\rho,\ V,\ u,\ P,\ E$ denotes the initial values upstream (ahead of the shock front), and the subscript "s" corresponds to the values downstream, in the shocked matter. It is most convenient to work in the reference frame where the front is at rest. Then the speed of the shock D is just u_0, because by definition it is measured relative to the unshocked matter.

Now $F_3 = \text{const}$ gives:

$$\left(E_0 + \frac{1}{2}j^2V_0 + P_0\right)u_0 = \left(E_s + \frac{1}{2}j^2V_s + P_s\right)u_s$$

If we make the replacement here of $u_i = jV_i$, we get:

$$\left(E_0 + \frac{1}{2}j^2V_0 + P_0\right)jV_0 = \left(E_s + \frac{1}{2}j^2V_s + P_s\right)jV_s\ .$$

From here

$$E_0V_0 + \frac{1}{2}j^2V_0^2 + P_0V_0 = E_sV_s + \frac{1}{2}j^2V_s^2 + P_sV_s\ ,$$

and

$$(E_0 + P_0)V_0 + \frac{1}{2}j^2(V_0^2 - V_s^2) = (E_s + P_s)V_s\ .$$

But $(V_0^2 - V_s^2) = (V_0 - V_s)(V_0 + V_s)$ and $P_s = P_0 + j^2(V_0 - V_s)$ obtained above implies $V_0 - V_s = (P_s - P_0)/j^2$, therefore j^2 cancels in the numerator and denominator:

$$(E_0 + P_0)V_0 + \frac{1}{2}\cancel{j^2}\frac{(P_s - P_0)}{\cancel{j^2}}(V_0 + V_s) = (E_s + P_s)V_s\ .$$

Thus

$$\left(E_0 + \frac{P_0 + P_s}{2}\right)V_0 = \left(E_s + \frac{P_0 + P_s}{2}\right)V_s\ ,$$

and we obtain a general formula for the compression in the flow (e.g., on a shock front):

$$\frac{V_s}{V_0} = \frac{2E_0 + P_0 + P_s}{2E_s + P_0 + P_s}\ .$$

An equation of state $E = E(P, V)$, or $P = P(E, V)$, gives the shock adiabat. For a general equation of state in a strong shock ($P_s \gg P_0,\ E_s \gg E_0$), which is most important in supernova envelopes,

$$\frac{V_s}{V_0} = \frac{2E_0/(P_0 + P_s) + 1}{2E_s/(P_0 + P_s) + 1} \approx \frac{1}{2E_s/P_s + 1} ,$$

or

$$\frac{\rho_s}{\rho_0} = \frac{V_0}{V_s} \approx 1 + \frac{2E_s}{P_s} ,$$

in the general case, and

$$\frac{\rho_s}{\rho_0} = \frac{V_0}{V_s} \approx 1 + \frac{2}{\gamma - 1} = \frac{\gamma + 1}{\gamma - 1} ,$$

for the case of an equation of state with $\gamma = \text{const}$.

Let $P = (\gamma - 1)E_{\text{tr}}$, where E_{tr} is the translational internal energy, that is, the kinetic energy of the particles in plasma, and let $E = E_{\text{tr}} + Q$, where Q is, for example, the ionisation potential energy. Then in a strong shock

$$\frac{\rho_s}{\rho_0} = \frac{V_0}{V_s} \approx 1 + \frac{2E_{2\text{tr}} + 2Q}{P_s} = 1 + \frac{2}{\gamma - 1} + \frac{2Q}{(\gamma - 1)E_{2\text{tr}}} ,$$

that is

$$\frac{\rho_s}{\rho_0} = \frac{V_0}{V_s} \approx \frac{\gamma + 1}{\gamma - 1} + \frac{2Q}{(\gamma - 1)E_{2\text{tr}}} .$$

For $\gamma = 5/3$ this gives

$$\frac{\rho_s}{\rho_0} = \frac{V_0}{V_s} \approx 4 + \frac{3Q}{E_{2\text{tr}}} .$$

This is formula (3.71) in Zeldovich and Raizer.

We found from the conservation of momentum ($F_2 = \text{const}$) that $P_s = P_0 + j^2(V_0 - V_s)$; that is,

$$j^2 = \frac{P_s - P_0}{V_0 - V_s} \approx \frac{P_s}{V_0 - V_s} = \frac{P_s}{V_0[1 - (\gamma - 1)/(\gamma + 1)]} = \frac{P_s(\gamma + 1)}{2V_0} ,$$

This is valid for a strong shock, constant γ, and small Q. Hence,

$$\rho_0 u_0^2 = \frac{P_s(\gamma + 1)}{2} ,$$

that is,

$$P_s = \frac{2}{\gamma + 1}\rho_0 u_0^2. \tag{11}$$

Note that γ here must be taken for the gas behind the strong shock in as much as the pressure P_0 is negligible and its equation of state is irrelevant.

For a nonrelativistic plasma with pressure $P = \mathscr{R}\rho T/\mu$ we get from (11)

$$\rho_0 u_0^2 = \frac{(\gamma+1)\mathscr{R}\rho_s T_s}{2\mu} ,$$

so

$$u_0^2 = \frac{(\gamma+1)\mathscr{R}\rho_s T_s}{2\rho_0\mu} = \frac{(\gamma+1)^2\mathscr{R}T_s}{2(\gamma-1)\mu} .$$

The post-shock temperature T_s for the strong shock, constant γ, and small Q is (from the last equation)

$$T_s = \frac{2(\gamma-1)u_0^2\mu}{(\gamma+1)^2\mathscr{R}} .$$

For $\gamma = 5/3$ we get

$$T_s = \frac{3u_0^2\mu}{16\mathscr{R}} . \tag{12}$$

If we put here $D_8 = u_0/10^8$ cm/s, then D_8 is the shock speed in units of 1000 km/s and we get

$$T_s(\mathrm{K}) = 2.25\times 10^7 \mu D_8^2 \tag{13}$$

in Kelvins or

$$T_s(\mathrm{keV}) = 1.94\mu D_8^2 \tag{14}$$

in keV. Here $\mu = A/(1+Z)$ for plasma (because $n = n_{\mathrm{baryon}}/\mu = n_{\mathrm{ion}}A/\mu = n_{\mathrm{ion}} + n_e = n_{\mathrm{ion}} + Zn_{\mathrm{ion}}$). Note that a typical value for D in SNe is about 10,000 km/s, thus T will be of order 10^9 K or hundreds of keV.

$\mathscr{R} \approx k_B/m_p$ where m_p is the proton mass, therefore we have

$$k_B T_s \sim m_p D_s^2. \tag{15}$$

This estimate is the same as that used in Sect. 3.2, Eq. (10) if we put $m_i = m_p$.

Using $\gamma = \mathrm{const}$ is a favourite approximation in many papers and simulations in astrophysics, but in supernovae it is a very bad one, and almost irrelevant. The value of γ varies because of the ionisation/excitation of the atoms. It changes a great deal on the shock front when it goes through the cold layers and heats the plasma so strongly that radiation pressure dominates downstream behind the front. In that case

(which is quite general for supernova shock breakout) the formulas (13) and (14) are not applicable and even misleading. The equations for mass, momentum, and energy conservation are more complicated for radiative shock waves when one has to account for the transfer of the momentum and energy of the photons. Nevertheless there are two important limiting cases for strong shocks with radiation, when simple expressions can be derived.

In the first limiting case, we may have relatively cold gas upstream with $P_0 \ll P_s$ in the strong shock, and the gas downstream is opaque with the pressure dominated by radiation.

Due to the high heat capacity of photon gas, the temperature behind the front is orders of magnitude lower than in Eqs. (13) and (14), and may be estimated as in Sect. 3.2.

Let us put radiation pressure for P_s into Eq. (11), we get

$$\frac{aT_s^4}{3} = \frac{2}{\gamma+1}\rho_0 u_0^2. \tag{16}$$

We have $\gamma = 4/3$ for the radiation-dominated gas, and, substituting $u_0 = D$, we obtain

$$T_s = \left(\frac{18}{7a}\rho_0 D^2\right)^{1/4}. \tag{17}$$

That is,

$$T_s(K) = 4.3 \times 10^4 \rho_{-12}^{1/4} D_8^{1/2}, \tag{18}$$

$\rho \sim 10^{-12}$ g $\cdot$ cm^{-3}, if we normalise density for $\rho = 10^{-12}$ g $\cdot$ cm^{-3} and take D in units of 1000 km/s. One can see that the shock temperature in reality is much less than in (14).

The second important limiting case takes place when the radiation is not trapped, and its pressure and momentum may be neglected, but when it is very efficient in heat transport. Now the energy is not conserved, and the energy flux F_3 is no longer constant. Instead of this, we may have the constancy of temperature ahead and behind the front. Mass and momentum conservation give as before:

$$P_s = P_0 + j^2(V_0 - V_s). \tag{19}$$

Now, both upstream and downstream the pressure is $P = \mathscr{R}\rho T/\mu$ with the same T, thus the strong shock condition, $P_s \gg P_0$ means not a high T behind the front, but $\rho_s \gg \rho_0$. $P_s \approx \rho_0 u_0^2$, which we get from (19), gives

$$\frac{\rho_s}{\rho_0} = \frac{\mu D^2}{\mathscr{R}T}. \tag{20}$$

The isothermal temperature T here is much less than the temperature found in Eqs. (13) and (14) for adiabatic shocks, hence the compression in isothermal shocks may be orders of magnitude larger than the canonical $(\gamma + 1)/(\gamma - 1)$ of adiabatic shocks. This is a typical situation for the formation of cool dense shells in interacting supernovae. The exact values of T and of the compression depend on the details of the properties of plasma with respect to heat conduction, but one should remember that those dense shells may become unstable, and the exact numbers found in idealised, accurately plane parallel or spherically symmetric calculations may not be very useful.

5 Conclusions

Interacting supernovae manifest themselves through many peculiar features in their spectra, and through powerful X-ray and/or radio emission. The most important effect of the interaction between SN ejecta and the circumstellar medium is the production of light by radiating shock waves. Many (but not all) superluminous supernovae may be explained by this mechanism.

6 Cross-References

▸ Interacting Supernovae: Types IIn and Ibn

Acknowledgements The work was supported by a grant from the Russian Science Foundation, 14-12-00203. The author is grateful to colleagues at ITEP, INASAN, Kavli IPMU, SAI MSU, NSU, VNIIA, FTI, and MPA for numerous discussions and collaborations.

References

Barkov MV (2012) Close binary progenitors of hypernovae. Int J Mod Phys Conf Ser 8:209–219. doi:10.1142/S2010194512004618

Benetti S (2000) Interacting Type II supernovae & Type IId. Mem. Soc. Astron. It. 71:323–329

Benetti S, Nicholl M, Cappellaro E, Pastorello A, Smartt SJ, Elias-Rosa N, Drake AJ, Tomasella L, Turatto M, Harutyunyan A, Taubenberger S, Hachinger S, Morales-Garoffolo A, Chen TW, Djorgovski SG, Fraser M, Gal-Yam A, Inserra C, Mazzali P, Pumo ML, Sollerman J, Valenti S, Young DR, Dennefeld M, Le Guillou L, Fleury M, Léget PF (2014) The supernova CSS121015:004244+132827: a clue for understanding superluminous supernovae. MNRAS 441:289–303. doi:10.1093/mnras/stu538, 1310.1311

Bose S, Sutaria F, Kumar B, Duggal C, Misra K, Brown PJ, Singh M, Dwarkadas V, York DG, Chakraborti S, Chandola HC, Dahlstrom J, Ray A, Safonova M (2015) SN 2013ej: a Type IIL supernova with weak signs of interaction. ApJ 806:160. doi:10.1088/0004-637X/806/2/160, 1504.06207

Chandra P, Chevalier RA, Chugai N, Fransson C, Soderberg AM (2015) X-ray and radio emission from Type IIn supernova SN 2010jl. ApJ 810:32. doi:10.1088/0004-637X/810/1/32, 1507.06059

Chevalier RA (1981) Hydrodynamic models of supernova explosions. Fundam Cosmic Phys 7: 1–58
Chevalier RA (1982a) Self-similar solutions for the interaction of stellar ejecta with an external medium. ApJ 258:790–797. doi:10.1086/160126
Chevalier RA (1982b) The radio and X-ray emission from Type II supernovae. ApJ 259:302–310. doi:10.1086/160167
Chevalier RA (2012) Common envelope evolution leading to supernovae with dense interaction. ApJ 752:L2. doi:10.1088/2041-8205/752/1/L2, 1204.3300
Chugai NN (1997a) Supernovae in dense winds. Astrophys Space Sci 252:225–236
Chugai NN (1997b) The origin of supernovae with dense winds. Astron Rep 41:672–681
Chugai NN (2009) Circumstellar interaction in Type Ibn supernovae and SN 2006jc. MNRAS 400:866–874. doi:10.1111/j.1365-2966.2009.15506.x, 0908.0568
Chugai NN, Chevalier RA, Utrobin VP (2007) Optical signatures of circumstellar interaction in Type IIP supernovae. ApJ 662:1136–1147. doi:10.1086/518160, astro-ph/0703468
Dwarkadas VV (2011) On luminous blue variables as the progenitors of core-collapse supernovae, especially Type IIn supernovae. MNRAS 412:1639–1649. doi:10.1111/j.1365-2966.2010.18001.x, 1011.3484
Dwarkadas VV, Gruszko J (2012) What are published X-ray light curves telling us about young supernova expansion? MNRAS 419:1515–1524. doi:10.1111/j.1365-2966.2011.19808.x, 1109.2616
Foley RJ, Smith N, Ganeshalingam M, Li W, Chornock R, Filippenko AV (2007) SN 2006jc: a Wolf-Rayet star exploding in a dense He-rich circumstellar medium. ApJ 657:L105–L108. doi:10.1086/513145, astro-ph/0612711
Grasberg EK, Nadezhin DK (1986) Type-II supernovae – two successive explosions. Sov Astron Lett 12:68–70
Heger A, Woosley SE (2002) The nucleosynthetic signature of population III. ApJ 567:532–543. doi:10.1086/338487, astro-ph/0107037
Immler S, Fesen RA, Van Dyk SD, Weiler KW, Petre R, Lewin WHG, Pooley D, Pietsch W, Aschenbach B, Hammell MC, Rudie GC (2005) Late-time X-ray, UV, and optical monitoring of supernova 1979C. ApJ 632:283–293. doi:10.1086/432869, astro-ph/0503678
Immler S, Modjaz M, Landsman W, Bufano F, Brown PJ, Milne P, Dessart L, Holland ST, Koss M, Pooley D, Kirshner RP, Filippenko AV, Panagia N, Chevalier RA, Mazzali PA, Gehrels N, Petre R, Burrows DN, Nousek JA, Roming PWA, Pian E, Soderberg AM, Greiner J (2008) Swift and Chandra detections of supernova 2006jc: evidence for interaction of the supernova shock with a circumstellar shell. ApJ 674:L85–L88. doi:10.1086/529373, 0712.3290
Inserra C, Turatto M, Pastorello A, Pumo ML, Baron E, Benetti S, Cappellaro E, Taubenberger S, Bufano F, Elias-Rosa N, Zampieri L, Harutyunyan A, Moskvitin AS, Nissinen M, Stanishev V, Tsvetkov DY, Hentunen VP, Komarova VN, Pavlyuk NN, Sokolov VV, Sokolova TN (2012) The bright Type IIP SN 2009bw, showing signs of interaction. MNRAS 422:1122–1139. doi:10.1111/j.1365-2966.2012.20685.x, 1202.0659
Justham S, Podsiadlowski P, Vink JS (2014) Luminous blue variables and superluminous supernovae from binary mergers. ApJ 796:121. doi:10.1088/0004-637X/796/2/121, 1410.2426
Kankare E, Ergon M, Bufano F, Spyromilio J, Mattila S, Chugai NN, Lundqvist P, Pastorello A, Kotak R, Benetti S, Botticella MT, Cumming RJ, Fransson C, Fraser M, Leloudas G, Miluzio M, Sollerman J, Stritzinger M, Turatto M, Valenti S (2012) SN 2009kn – the twin of the Type IIn supernova 1994W. MNRAS 424:855–873. doi:10.1111/j.1365-2966.2012.21224.x, 1205.0353
Leloudas G, Hsiao EY, Johansson J, Maeda K, Moriya TJ, Nordin J, Petrushevska T, Silverman JM, Sollerman J, Stritzinger MD, Taddia F, Xu D (2015) Supernova spectra below strong circumstellar interaction. A&A 574:A61. doi:10.1051/0004-6361/201322035, 1306.1549
Margutti R, Milisavljevic D, Soderberg AM, Chornock R, Zauderer BA, Murase K, Guidorzi C, Sanders NE, Kuin P, Fransson C, Levesque EM, Chandra P, Berger E, Bianco FB, Brown PJ, Challis P, Chatzopoulos E, Cheung CC, Choi C, Chomiuk L, Chugai N, Contreras C, Drout MR, Fesen R, Foley RJ, Fong W, Friedman AS, Gall C, Gehrels N, Hjorth J, Hsiao E, Kirshner R, Im M, Leloudas G, Lunnan R, Marion GH, Martin J, Morrell N, Neugent KF, Omodei N,

Phillips MM, Rest A, Silverman JM, Strader J, Stritzinger MD, Szalai T, Utterback NB, Vinko J, Wheeler JC, Arnett D, Campana S, Chevalier R, Ginsburg A, Kamble A, Roming PWA, Pritchard T, Stringfellow G (2014) A panchromatic view of the restless SN 2009ip reveals the explosive ejection of a massive star envelope. ApJ 780:21. doi:10.1088/0004-637X/780/1/21, 1306.0038

Margutti R, Kamble A, Milisavljevic D, Zapartas E, de Mink SE, Drout M, Chornock R, Risaliti G, Zauderer BA, Bietenholz M, Cantiello M, Chakraborti S, Chomiuk L, Fong W, Grefenstette B, Guidorzi C, Kirshner R, Parrent JT, Patnaude D, Soderberg AM, Gehrels NC, Harrison F (2017) Ejection of the massive hydrogen-rich envelope timed with the collapse of the stripped SN 2014C. ApJ 835:140. doi:10.3847/1538-4357/835/2/140, 1601.06806

Moriya TJ (2014) Mass loss of massive stars near the Eddington luminosity by core neutrino emission shortly before their explosion. A&A 564:A83. doi:10.1051/0004-6361/201322992, 1403.2731

Moriya TJ, Maeda K, Taddia F, Sollerman J, Blinnikov SI, Sorokina EI (2014) Mass-loss histories of Type IIn supernova progenitors within decades before their explosion. MNRAS 439: 2917–2926. doi:10.1093/mnras/stu163, 1401.4893

Nadezhin DK (1985) On the initial phase of interaction between expanding stellar envelopes and surrounding medium. Astrophys Space Sci 112:225–249. Preprint ITEP-1, 1981, doi:10.1007/BF00653506

Nomoto K, Suzuki T, Deng J, Uenishi T, Hachisu I (2005) Progenitors of Type Ia supernovae: circumstellar interaction, rotation, and steady hydrogen burning. In: Turatto M, Benetti S, Zampieri L, Shea W (eds) 1604-2004: supernovae as cosmological lighthouses. Astronomical Society of the Pacific conference series, vol 342, p 105. astro-ph/0603432

Ofek EO, Zoglauer A, Boggs SE, Barriére NM, Reynolds SP, Fryer CL, Harrison FA, Cenko SB, Kulkarni SR, Gal-Yam A, Arcavi I, Bellm E, Bloom JS, Christensen F, Craig WW, Even W, Filippenko AV, Grefenstette B, Hailey CJ, Laher R, Madsen K, Nakar E, Nugent PE, Stern D, Sullivan M, Surace J, Zhang WW (2014) SN 2010jl: optical to hard X-ray observations reveal an explosion embedded in a ten solar mass Cocoon. ApJ 781:42. doi:10.1088/0004-637X/781/1/42, 1307.2247

Pastorello A, Smartt SJ, Mattila S, Eldridge JJ, Young D, Itagaki K, Yamaoka H, Navasardyan H, Valenti S, Patat F, Agnoletto I, Augusteijn T, Benetti S, Cappellaro E, Boles T, Bonnet-Bidaud JM, Botticella MT, Bufano F, Cao C, Deng J, Dennefeld M, Elias-Rosa N, Harutyunyan A, Keenan FP, Iijima T, Lorenzi V, Mazzali PA, Meng X, Nakano S, Nielsen TB, Smoker JV, Stanishev V, Turatto M, Xu D, Zampieri L (2007) A giant outburst two years before the core-collapse of a massive star. Nature 447:829–832. doi:10.1038/nature05825, astro-ph/0703663

Pastorello A, Wang XF, Ciabattari F, Bersier D, Mazzali PA, Gao X, Xu Z, Zhang JJ, Tokuoka S, Benetti S, Cappellaro E, Elias-Rosa N, Harutyunyan A, Huang F, Miluzio M, Mo J, Ochner P, Tartaglia L, Terreran G, Tomasella L, Turatto M (2016) Massive stars exploding in a He-rich circumstellar medium - IX. SN 2014av, and characterization of Type Ibn SNe. MNRAS 456:853–869. doi:10.1093/mnras/stv2634, 1509.09069

Quimby RM, Kulkarni SR, Kasliwal MM, Gal-Yam A, Arcavi I, Sullivan M, Nugent P, Thomas R, Howell DA, Nakar E, Bildsten L, Theissen C, Law NM, Dekany R, Rahmer G, Hale D, Smith R, Ofek EO, Zolkower J, Velur V, Walters R, Henning J, Bui K, McKenna D, Poznanski D, Cenko SB, Levitan D (2011) Hydrogen-poor superluminous stellar explosions. Nature 474:487–489. doi:10.1038/nature10095, 0910.0059

Raskin C, Kasen D (2013) Tidal tail ejection as a signature of Type Ia supernovae from white dwarf mergers. ApJ 772:1. doi:10.1088/0004-637X/772/1/1, 1304.4957

Salamanca I (2003) The dense circumstellar material around Type IIn supernovae. In: Perez E, Gonzalez Delgado RM, Tenorio-Tagle G (eds) Star formation through time. Astronomical Society of the Pacific conference series, vol 297. Astronomical Society of the Pacific, San Francisco, p 429

Schlegel EM, Kirshner RP, Huchra JP, Schild RE (1996) The peculiar Type II SN 1987B in NGC 5850. AJ 111:2038. doi:10.1086/117939

Shiode JH, Quataert E (2014) Setting the stage for circumstellar interaction in core-collapse supernovae. II. Wave-driven mass loss in supernova progenitors. ApJ 780(1):96. http://stacks.iop.org/0004-637X/780/i=1/a=96

Smith N (2014) Mass loss: its effect on the evolution and fate of high-mass stars. ARA&A 52: 487–528. doi:10.1146/annurev-astro-081913-040025, 1402.1237

Smith N, Hinkle KH, Ryde N (2009) Red supergiants as potential Type IIn supernova progenitors: spatially resolved 4.6 μm CO emission around VY CMa and betelgeuse. AJ 137:3558–3573. doi:10.1088/0004-6256/137/3/3558, 0811.3037

Sorokina E, Blinnikov S, Nomoto K, Quimby R, Tolstov A (2016) Type I superluminous supernovae as explosions inside non-hydrogen circumstellar envelopes. ApJ 829:17. doi:10.3847/0004-637X/829/1/17, 1510.00834

Turatto M (2003) Classification of supernovae. In: Weiler K (ed) Supernovae and gamma-ray bursters. Lecture notes in physics, vol 598. Springer, Berlin, pp 21–36. astro-ph/0301107

Utrobin VP, Chugai NN (2015) Parameters of Type IIP SN 2012A and clumpiness effects. A&A 575:A100. doi:10.1051/0004-6361/201424822, 1411.6480

Valenti S, Sand D, Stritzinger M, Howell DA, Arcavi I, McCully C, Childress MJ, Hsiao EY, Contreras C, Morrell N, Phillips MM, Gromadzki M, Kirshner RP, Marion GH (2015) Supernova 2013by: a Type IIL supernova with a IIP-like light-curve drop. MNRAS 448: 2608–2616. doi:10.1093/mnras/stv208, 1501.06491

Woosley SE, Blinnikov S, Heger A (2007) Pulsational pair instability as an explanation for the most luminous supernovae. Nature 450:390–392. doi:10.1038/nature06333, 0710.3314

Yoshida T, Umeda H, Maeda K, Ishii T (2016) Mass ejection by pulsational pair instability in very massive stars and implications for luminous supernovae. MNRAS 457:351–361. doi:10.1093/mnras/stv3002, 1511.01695